Dalton Transactions

PAPER

View Article Online
View Journal | View Issue

Cite this: *Dalton Trans.*, 2016, **45**, 11384

Cationic 5-phosphonio-substituted N-heterocyclic carbenes†

Kai Schwedtmann,[a] Robin Schoemaker,[a] Felix Hennersdorf,[a] Antonio Bauzá,[b] Antonio Frontera,[b] Robert Weiss[c] and Jan J. Weigand*[a]

Received 11th May 2016,
Accepted 3rd June 2016

DOI: 10.1039/c6dt01871h

www.rsc.org/dalton

2-Phosphanyl-substituted imidazolium salts 2-PR_2(4,5-Cl-Im)[OTf] (**9a,b**[OTf]) (4,5-Cl-Im = 4,5-dichloro-1,3-bis(2,6-di-isopropylphenyl)-imidazolium) (a: R = Cy, b: R = Ph) are prepared from the reaction of R_2PCl (R = Cy, Ph) with NHC **8** (4,5-dichloro-1,3-bis(2,6-di-isopropylphenyl)-imidazolin-2-ylidene) in the presence of Me_3SiOTf. 5-Phospanyl-substituted imidazolium salts 5-PR_2(2,4-Cl-Im)[OTf] (**10a,b**[OTf]) are obtained in quantitative yield when a slight excess of the NHC **8** is used. 5-Phosphonio-substituted imidazolium salts 5-PR_2Me(2,4-Cl-Im)$[OTf]_2$ (**14a,b**$[OTf]_2$) and 5-PR_2F(2,4-Cl-Im)$[OTf]_2$ (**16a,b**$[OTf]_2$) result from methylation reaction or oxidation of **10a,b**[OTf] with XeF_2 and subsequent fluoride abstraction. According to our quantum chemical studies the Cl1 atom at the 2-position at the imidazolium ring of dication **14b**$^{2+}$ carries a slightly positive charge and is therefore accessible for nucleophilic attack. Accordingly, the reaction of **14a,b**$[OTf]_2$ and **16a,b**$[OTf]_2$ with R_3P (R = Cy, Ph) affords cationic 5-phosphonio-substituted NHCs 5-PR_2Me(4-Cl-NHC)[OTf] (**17a,b**[OTf]) and 5-PR_2F(4-Cl-NHC)[OTf] (**18a,b**[OTf]) *via* a S_N2(Cl)-type reaction. A series of transition metal complexes such as [AuCl(5-PPh_2Me(4-Cl-NHC))][OTf] (**19**[OTf]), [CuBr(5-PPh_2Me(4-Cl-NHC))][OTf] (**20**[OTf]), [AuCl(5-PPh_2F(4-Cl-NHC))[OTf] (**21**[OTf]) and [RhCl(cod)(5-PPh_2Me(4-Cl-NHC))][OTf] (**23**[OTf]) are prepared to prove the coordination abilities of carbenes **17b**[OTf] and **18b**[OTf]. The isolation of a rare example of a tricationic bis-carbene silver complex [Ag(5-PPh_2Me(4-Cl-NHC))$_2$]$[OTf]_3$ (**22**$[OTf]_3$) is achieved by reacting **14b**[OTf] with Cy_3P in the presence of AgOTf. NHC **17b**[OTf] represents a very effective dehydrocoupling reagent for secondary (R_2PH, R = Ph, Cy, ^{i}Bu) and primary (RPH_2, R = Ph, Cy) phosphanes to give diphosphanes of type R_4P_2 (R = Ph, Cy, ^{i}Bu) and oligophosphanes R_4P_4, R_5P_5 (R = Ph, Cy), respectively. Methylation of **17b**$^+$ and subsequent deprotonation reaction with LDA affords the cationic NHO (N-heterocyclic olefin) **35**$^+$ of which the gold complex **36**$^+$ is readily accessible *via* the reaction with AuCl(tht).

Introduction

The application of N-heterocyclic carbenes (NHCs) in phosphorus chemistry has led to some remarkable discoveries in recent years and is a growing field with considerable impact. The most general feature of NHCs is their tendency to react at the 2-position with electrophilic P^{III} compounds, leading to the corresponding 2-phosphanyl-substituted imidazolium salts or to donor–acceptor complexes of the NHC and the respective P-centered moiety.[1,2] In contrast, only a few examples are known where the 4/5-position of NHCs can be selectively addressed to yield 4/5-phosphanyl-substituted NHCs or imidazolium salts. Reactions are reported involving *inter alia* phosphaalkenes[3] and chlorophosphanes.[4,5] In 2009 Gates and coworkers observed the unusual reaction of 1,3-di(mesityl)imidazolin-2-ylidene **1** with phosphaalkene MesP=CPh_2 to afford the first example of a neutral 4-phosphanyl-substituted NHC **2** (Scheme 1, top).[3] Shortly afterwards, Bertrand and coworkers observed the rearrangement reaction of 2-phosphanyl-substituted imidazolium salt **3**[Cl] to the 4-substituted derivative **4** when treated with a base (*e.g.* KHMDS; Scheme 1, middle).[4] The neutral 4-phosphanyl-substituted NHCs **2** and **4** were used as ligands in transition metal chemistry to generate mono metallic,[6] homo-[6,7] and hetero-[7] bimetallic complexes. In 2013 our group reported on the reaction of P-centered imidazolium salt **5**[OTf] with NHC **6** leading to the cationic phosphoranide derivative **7**[OTf] where the second imidazoliumyl-substituent is bonded *via* the 4-position to the P atom (Scheme 1, bottom). The proposed mechanism

---

[a] *Department of Chemistry and Food Chemistry, TU Dresden, 01062 Dresden, Germany. E-mail: jan.weigand@tu-dresden.de; Fax: (+49) 351-463-31478*
[b] *Department of Chemistry, Universitat de les Illes Balears, Palma de Mallorca, Spain*
[c] *Department of Chemistry and Pharmacy, Friedrich-Alexander-Universität Erlangen, 91054 Erlangen, Germany*

† Electronic supplementary information (ESI) available. CCDC 1450345–1450355, 1469786–1469788. For ESI and crystallographic data in CIF or other electronic format see DOI: 10.1039/c6dt01871h

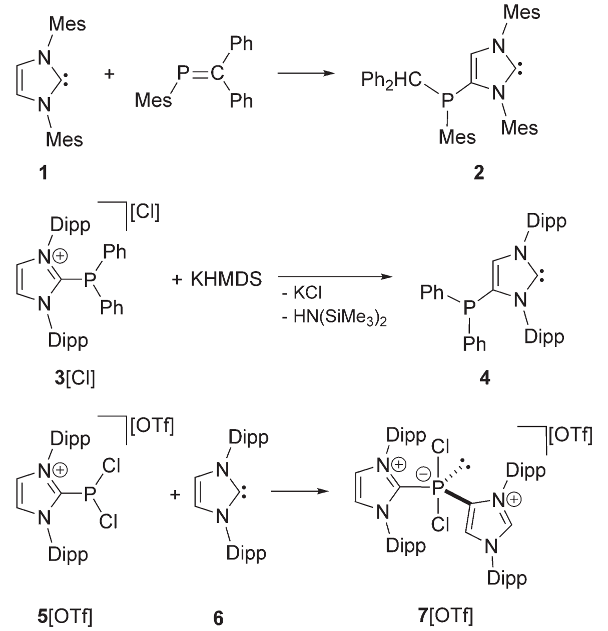

Scheme 1 Preparation of **2**, **4**, and **7**[OTf] (Mes = 1,3,5-trimethylphenyl, Dipp = 2,6-diisopropylphenyl, Ph = phenyl, HMDS = bis(trimethylsilyl) amide); for all examples, only one representative Lewis structure is depicted.

includes the formation of an *abnormal* carbene[8] followed by an intermolecular rearrangement, which we believe is related to Bertrand's mechanism for the formation of **4**.[4]

Only very few examples of 4-, 4,5-bisphosphoryl-[9] and 4,5-bis-phosphanyl-[10] substituted imidazolium salts and 4-phosphanido-substituted NHC[11] are reported in the literature so far. The aforementioned compounds exhibit either one or two Lewis basic functionalities. However, so far there is no example of a cationic NHC featuring a phosphonium functionality at the 4/5-position, which should have a significant influence on the reactivity of the carbene.

Results and discussion

The reaction of chlorophosphanes R_2PCl (R = Cy, Ph) with Me_3SiOTf and NHC **8**[12] in a precise 1 : 1 : 1 reaction gives the corresponding 2-phosphanyl-substituted imidazolium salts **9a**, **b**[OTf] in excellent yield (**9a**[OTf]: 91%; **9b**[OTf]: 99%; Scheme 2). The ^{31}P NMR spectra of the purified, colorless solids show a singlet resonance in each case (**9a**$^+$: $\delta(P)$ = 12.7 ppm; **9b**$^+$: $\delta(P) = -5.1$ ppm), which is significantly upfield shifted compared to the respective chlorophosphanes (Cy_2PCl: $\delta(P)$ = 127.1 ppm; Ph_2PCl: $\delta(P)$ = 81.9 ppm)[13] due to the presence of the imidazolium substituents. Suitable single crystals for X-ray analysis are obtained by slow diffusion of *n*-hexane into a saturated CH_2Cl_2 solution of **9b**[OTf] (Fig. 1). The P–C bond lengths (P–C1 1.8437(9) Å, P–C28 1.8205(10) Å, P–C34 1.8249(10) Å) are in the expected range of a P–C single bond (1.83 Å) involving a tri-coordinate phosphorus atom.[14]

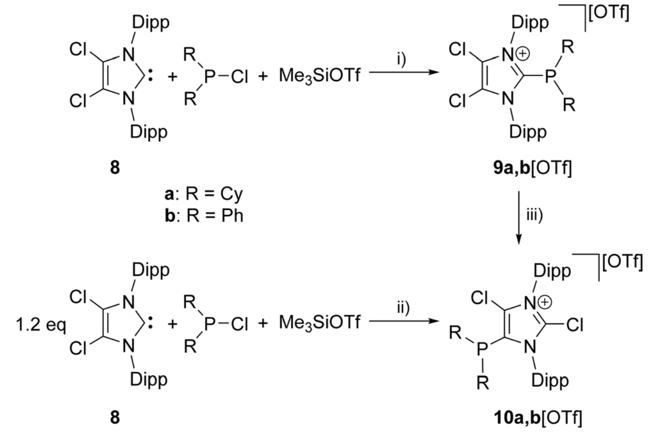

Scheme 2 Preparation of **9a,b**[OTf], (i): C_6H_5F, r.t., 6 h, **9a**[OTf] 91%; **9b**[OTf] 99%; preparation of **10a,b**[OTf]; (ii): *o*-$C_6H_4F_2$, r.t. 14 h, **10a**[OTf] 92%; **10b**[OTf] 97%; conversion of **9a,b**[OTf] to **10a,b**[OTf], (iii) 0.3 eq. 8, *o*-$C_6H_4F_2$, r.t. 30 h, quantitative.

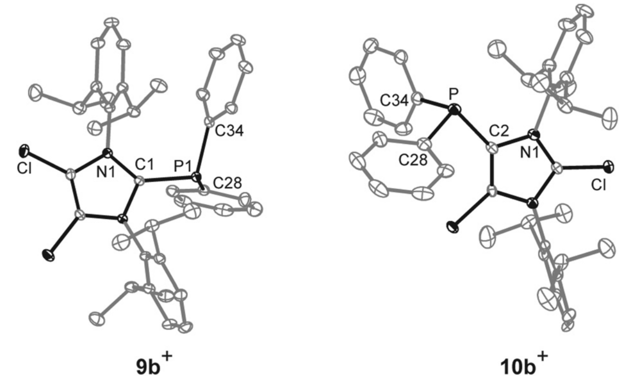

Fig. 1 Molecular structures of cations **9b**$^+$ and **10b**$^+$ of the respective triflate salts; hydrogen atoms, solvate molecules and anions are omitted for clarity and thermal ellipsoids are displayed at 50% probability; selected bond lengths (Å) and angles (°) for **9b**$^+$: P–C1 1.8437(9), P–C28 1.8205(10), P–C34 1.8249(10); C1–P–C28 107.15(4), C1–P–C34 100.59(4), C28–P–C34 101.71(4) and **10b**$^+$: P–C2 1.831(4), P–C28 1.827(4), P–C34 1.830(4); C2–P–C28 100.22(16), C2–P–C34 103.41(16), C28–P–C34 103.52(17).

Increasing the amount of NHC **8** to 1.2 equivalents in the reaction leads to the quantitative formation of 5-phosphanyl-substituted imidazolium salts **10a,b**[OTf] (**10a**[OTf]: 92%; **10b**[OTf]: 97%). The molecular structure of cation **10b**$^+$ is depicted in Fig. 1. The P–C bond lengths in this cation (P–C2 1.831(4) Å, P–C28 1.827(4) Å, P–C34 1.830(4) Å) are in the same range as those observed for the structural isomer **9b**$^+$ and compound **4** (P–C2 1.8124(12) Å, P–C_{Ph1} 1.8318(14) Å, P–C_{Ph2} 1.8388(13) Å). Compared to **9a,b**[OTf], a pronounced high field shift is observed in the ^{31}P NMR spectra for the 5-substituted derivatives **10a,b**[OTf] (**10a**$^+$: $\delta(P) = -15.2$ ppm; **10b**$^+$: $\delta(P) = -28.9$ ppm). This can be explained by the stronger σ-donor abilities of the carbon atom in the 5-position compared to the 2-position,[15–18] and the weaker electron withdrawing effect of only one N atom in β-position to the P atom. The ^1H NMR spectra of **10a,b**[OTf] show the expected additional sets of resonances for the isopropyl-groups of the Dipp-substituents due to a lower symmetry compared to **9a,b**[OTf] (see Fig. S2.1†). Compounds **9a,b**[OTf] are cleanly converted to the 5-substituted derivatives **10a,b**[OTf] within 30 h when adding 0.3 equivalents of NHC **8** to the dissolved material in $C_6H_4F_2$. The time dependent ^{31}P NMR spectra also confirm our suggestion that **9a,b**$^+$ is first formed and slowly converted into **10a,b**$^+$ during the reaction (Fig. 2). After 2 h, significant amounts of **9b**$^+$ are consumed along with the formation of the structural isomer **10b**$^+$ (**9b**$^+$: δ(P) = −5.1 ppm and **10b**$^+$: δ(P) = −28.9 ppm). The presence of two doublet resonances at δ(P) = −7.5 ppm and 30.7 ppm, (marked with a red and blue dot) with low intensity and a coupling constant of $^4J_{PP}$ = 7 Hz indicates the formation of intermediately formed cation **12b**$^+$ (Fig. 2). We thus propose for the rearrangement reaction for the first step a chlorenium ion abstraction from cation **9b**$^+$ by NHC **8** to give chloroimidazolium salt **8Cl**$^+$ and mesoionic NHC **11b** (Scheme 3). The latter reacts with **9b**$^+$ *via* phosphanyl-abstraction to NHC **8** and cation **12b**$^+$ whose formation is observed in the time dependent ^{31}P NMR spectra (Fig. 2). NHC **8** abstracts a PR$_2$-moiety from cation **12b**$^+$ to liberate cation **9b**$^+$ and intermediately formed NHC **13b**. The catalytic cycle is closed by the chlorenium ion abstraction from **8Cl**$^+$ by **13b** to yield 5-phosphanyl-substituted imidazolium cation **10b**$^+$ and catalyst NHC **8**. This catalytic cycle also explains the formation of cation **10a**$^+$ and is related to a mechanism we proposed recently elsewhere.[5]

The reaction of **10a,b**[OTf] with methyltriflate (MeOTf) in CH_2Cl_2 leads to the quantitative formation of the corresponding 5-phosphonium ions **14a,b**$^{2+}$ as triflate salts (isolated yield **14a**[OTf]$_2$: 68%; **14b**[OTf]$_2$: 79%; Scheme 4). This is indicated by a pronounced downfield shifted quartet resonance (**14a**$^{2+}$: δ(P) = 38.8 ppm, $^2J_{PH}$ = 12 Hz; **14b**$^{2+}$: δ(P) = 16.9 ppm, $^2J_{PH}$ = 14 Hz) in the respective ^{31}P NMR spectrum. Single crystals of **14b**$^+$ suitable for X-ray crystallography are obtained by slow diffusion of *n*-hexane into a saturated CH_2Cl_2 solution of **14b**[OTf]$_2$ (Fig. 3). The molecular structure of cation **14b**$^{2+}$ shows the expected tetra-coordinate bonding environment at the P atom and slightly shortened P–C bond distances (P–C2 1.810(2) Å, P–C28 1.782(2) Å, P–C34 1.787(2) Å, P–C40 1.790(2) Å) compared to cation **10b**$^+$. Selected geometrical parameters are given in Table 1.

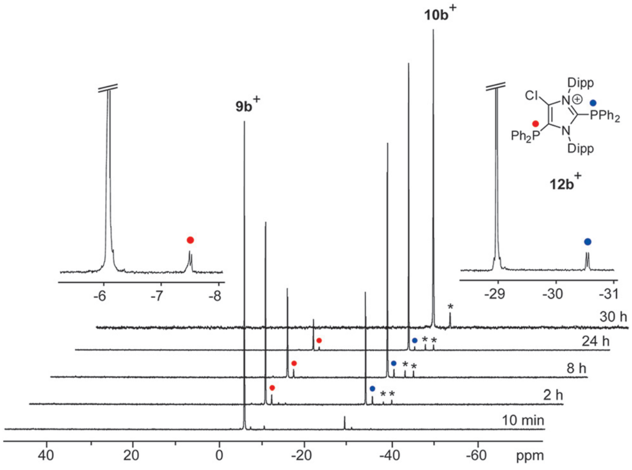

Fig. 2 Time-dependent ^{31}P NMR spectra for the reaction of **9b**[OTf] with 0.3 eq. of NHC **8** (o-$C_6H_4F_2$, C_6D_6-capillary, 300 K). The intermediately formed cation **12b**$^+$ is indicated by red and blue dots, not identified intermediates by asterisks.

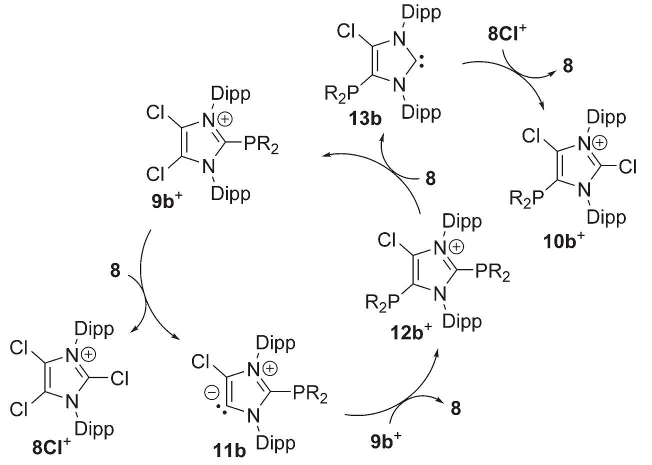

Scheme 3 Proposed mechanism for the formation of cations **10b**$^+$; anions are omitted for clarity.

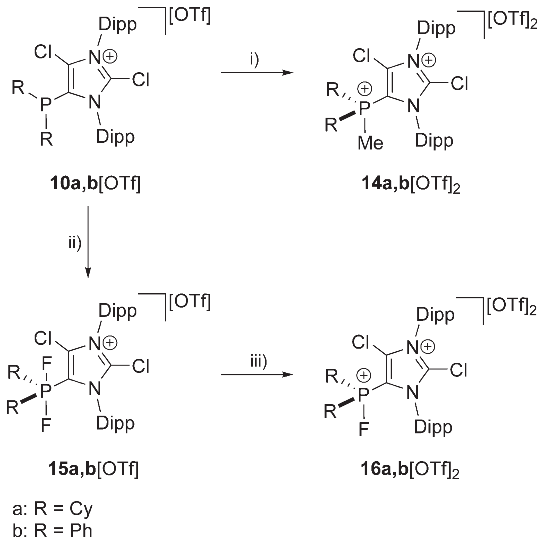

Scheme 4 Preparation of: **14a,b**[OTf]$_2$, (i): + MeOTf, C_6H_5F, r.t., 6 h, **14a**[OTf]$_2$: 68%; **14b**[OTf]$_2$: 79%; **15a,b**[OTf], (ii): +XeF$_2$, CH_2Cl_2, r.t. 2 h, −Xe, **15a**[OTf]: 81%; **15b**[OTf]: 89%; **16a,b**[OTf]$_2$, (iii): +Me$_3$SiOTf, o-$C_6H_4F_2$, r.t. 5 h, −Me$_3$SiF, **16a**[OTf]$_2$: 72%; **16b**[OTf]$_2$: 71%.

One of the oxygen atoms of one triflate anion shows a close contact to the Cl1 atom that is well within the sum of the van der Waals radii (O4⋯Cl1 2.813(2) Å; $r_{A(O)} + r_{A(Cl)}$ = 3.21 Å).[19] Also the almost linear C1–Cl1–O4 angle of 170.879(6)° is indicative for a strongly directional rather than purely electrostatic interaction, namely a halogen bonding.[20]

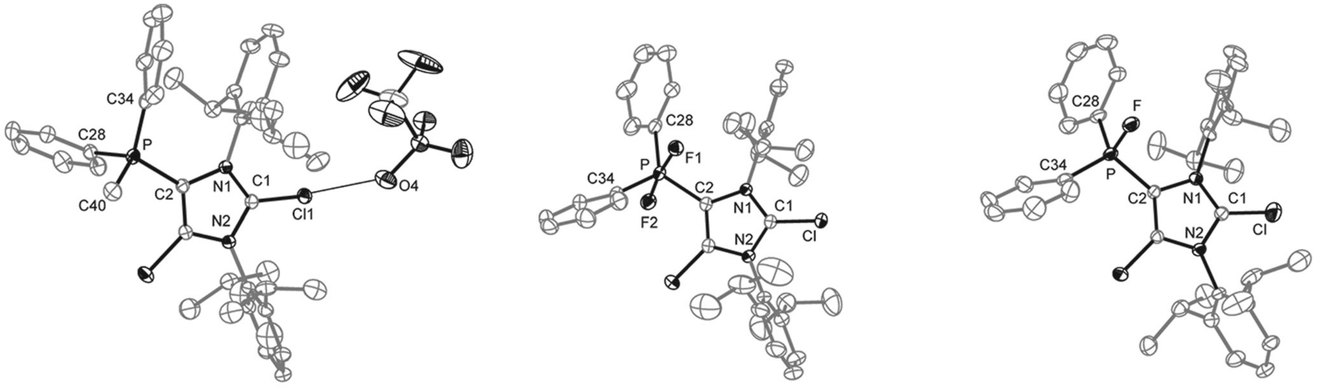

$14b^{2+}$ **$15b^{+}$** **$16b^{2+}$**

Fig. 3 Molecular structures of **$14b^{2+}$**, **$15b^{+}$**, and **$16b^{2+}$** of the respective triflate salts; hydrogen atoms, solvent molecules and anions are omitted for clarity and thermal ellipsoids are displayed at 50% probability. Selected geometrical parameters are given in Tables 1 and 2.

This effect might be attributed to a slightly increased electrophilic character of the Cl1 atom caused by the high group electronegativity of dication **$14b^{2+}$** (*vide infra*).[20–22]

The quantitative oxidation of **10a,b**[OTf] *via* the slow addition of a solution of XeF_2 in CH_2Cl_2 affords the difluorophosphoranes **15a,b**[OTf] (isolated yield >80%; Scheme 4). Analytically pure compounds are obtained *via* precipitation with *n*-hexane. For both compounds the ^{31}P NMR spectra show the expected triplet resonance with a typical $^1J_{PF}$ coupling due to the presence of two chemically equivalent fluorine atoms (**$15a^{+}$**: $\delta(P) = -28.6$ ppm, $^1J_{PF} = 722$ Hz; **$15b^{+}$**: $\delta(P) = -64.9$ ppm, $^1J_{PF} = 715$ Hz). Single crystals suitable for structure investigation are obtained by slow diffusion of *n*-hexane into a saturated CH_2Cl_2 solution of **15b**[OTf]. Cation **$15b^{+}$** shows a trigonal bipyramidal bonding environment at the P atom with the F atoms being in the axial positions displaying an almost linear F–P–F angle of 172.91(10)° and typical P–F bond lengths (P–F1 1.6523(19) Å, P–F2 1.6582(19) Å; Fig. 3).

In contrast to a related difluorophosphorane,[23] which requires a very strong fluoride abstracting reagent such as $Et_3Si[B(C_6F_5)_4]\cdot 2(C_7H_8)$, the reaction of **15a,b**[OTf] with Me_3SiOTf in CH_2Cl_2 quantitatively gives the fluorophosphonium salts **16a,b**[OTf]. Analytically pure compounds are obtained after the addition of *n*-hexane (isolated yield >70%). The ^{31}P NMR spectra of the isolated compounds display a pronounced downfield shifted doublet resonance (**$16a^{2+}$**: $\delta(P) = 109.6$ ppm, $^1J_{PF} = 988$ Hz; **$16b^{2+}$**: $\delta(P) = 70.5$ ppm, $^1J_{PF} = 995$ Hz), coinciding with the electron deficiency at the P atom as observed for similar Lewis acidic fluorophosphonium derivatives.[23,24] Accordingly, the much larger $^1J_{PF}$ coupling constant in **$16a,b^{2+}$** compared to **$15a,b^{+}$** results from a decreased electron density at the P atom.[25] The formation of dication **$16b^{2+}$** was also confirmed by X-ray crystallography (Fig. 3). The P–F bond (1.5612(19) Å) is substantially shortened compared to the P–F bond lengths in **$15b^{+}$** (*vide supra*), which is in agreement with the change of hybridization from sp^2 to sp^3 at the P atom. The same trend is observed for the P–C bonds to the phenyl substituents in **$16b^{2+}$** (P–C28 1.778(3) Å, P–C34 1.769(3) Å) compared to **$15b^{+}$** (P–C28 1.808(3) Å, P–C34 1.804(3) Å). Similarly, the P–C2 bond length in **$16b^{2+}$** (P–C2 1.782(3) Å) is significantly shortened compared to that in **$15b^{+}$** (P–C2 1.826(3) Å). Selected geometrical parameters are given in Table 2.

In order to shed light on the reactivity of dications **$14a,b^{2+}$** and **$16a,b^{2+}$** we analyzed the Merz–Kollman (M–K) and the Mulliken (Mull) charge distribution of **$14b^{2+}$** which are shown in Fig. 4 (left). Moreover, the Molecular Electrostatic Potential (MEP) distribution of **$14b^{2+}$** was calculated and plotted onto the van der Waals surface were regions of high charge are blue and regions with lower charge red (Fig. 4, right). For this study the geometries and energies were calculated applying the density functional theory (DFT) model BP86[26] with the latest correction of dispersion (D3),[27] together with the def2-TZVP basis set.[28,29] Both methods confirm a significant positive charge of the Cl atoms (Cl1: +0.41*e* (M–K), +0.12*e* (Mull); Cl2:

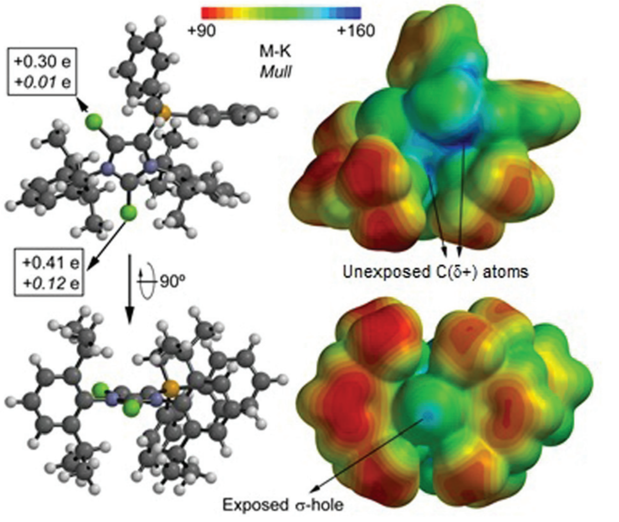

Fig. 4 Two orientations of cation **$14b^{2+}$** calculated at BP86-D3/def2-TZVP level of theory; Merz–Kollman (M–K) and the Mulliken (Mull, italics) charge distribution (left); Molecular Electrostatic Potential (MEP) distribution plotted onto the van der Waals surface (right).

+0.30*e* (M–K), +0.01*e* (Mull)) which are bonded to the imidazolium ring, whereas the Cl1 atom, bonded to the 2-position, is more positive. The MEP surface illustrates that the imidazolium ring has the highest charge, however, it is not accessible for a nucleophilic attack due to steric effects. In sharp contrast, the Cl1 atom is very exposed and presents a σ-hole – a well defined positively charged region on the extension of the C1–Cl1 bond.[20,30] Therefore, the most reactive site towards voluminous nucleophiles in dication **14b**$^{2+}$ is indeed the Cl1 atom bonded at the 2-position.

As for dications **14a,b**$^{2+}$ and **16a,b**$^{2+}$ we aimed at the synthesis of the corresponding cationic 5-phosphonio-substituted NHCs and proceeded to react dications **14a,b**$^{2+}$ and **16a,b**$^{2+}$ with Cy_3P or PPh_3, respectively (Scheme 5). The reaction of **14a,b**[OTf]$_2$ with Cy_3P in C_6H_5F gives quantitatively Cy_3PCl [OTf], of which the cation Cy_3PCl^+ was unambiguously identified by its ^{31}P NMR chemical shift of δ(P) = 104.2 ppm (ref. 31) in the reaction mixture. The ^{31}P NMR spectra of the reaction mixtures also show a second resonance which can be assigned to the cationic NHCs **17a,b**$^+$. The isolation of **17a**[OTf] was hampered due to a similar solubility of **17a**[OTf] and Cy_3PCl [OTf]. Analytically pure **17b**[OTf] was isolated as colorless powder in good yield (75%) *via* precipitation and washing with benzene. For cation **17b**$^+$ a slightly high field shifted singlet resonance in the ^{31}P NMR spectrum (δ(P) = 10.6 ppm) compared to **14b**$^{2+}$ (δ(P) = 16.9 ppm) is observed. The ^{13}C NMR spectrum displays a resonance at δ(C) = 230.2 ppm confirming the formation of an NHC.[16,32] This signal, which is downfield shifted compared to NHC **8** (δ(C) = 219.4 ppm, in C_6D_6),[12] splits into a doublet due to the coupling to the P atom in 5-position ($^3J_{CP}$ = 6 Hz). As compound **17b**[OTf] can be handled in solvents such as CH_2Cl_2 and CH_3CN without decomposition the scope of application is significantly broadened. Single crystals suitable for X-ray crystallography are obtained by slow diffusion of *n*-hexane into a saturated C_6H_5F solution of **17b**[OTf] (Fig. 5). Major differences in this cation compared to dication **14b**$^{2+}$ are the elongation of the C1–N1/N2 bond lengths (**17b**$^+$: C1–N1 1.375(3) Å, C1–N2 1.362(3) Å *vs.* **14b**$^{2+}$: C1–N1 1.335(2) Å, C1–N2 1.337(2) Å)) and the reduced bond angle N1–C1–N2 (**17b**$^+$: 102.40(16)° *vs.* **14b**$^{2+}$: N1–C1–N2 110.42(14)°). These effects are explained by a diminished π-delocalization[16,32] in the N1–C1–N2 moiety and an increased p-orbital character of the C1–N1/N2 bonds. As a result of the diminished π-delocalization within the imidazole ring the P–C2 bond length in **17b**$^+$ (1.779(2) Å) is significantly shortened compared to that in **14b**$^+$ (P–C2 1.810(2) Å). Selected geometrical parameters are summarized in Table 1.

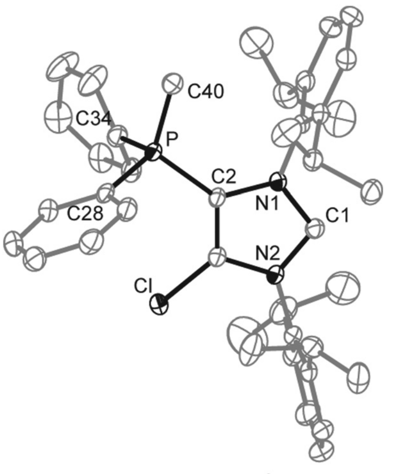

17b$^+$

Fig. 5 Molecular structure of **17b**$^+$ of the triflate salt; hydrogen atom and anions are omitted for clarity and thermal ellipsoids are displayed at 50% probability. Selected geometrical parameters are given in Table 1.

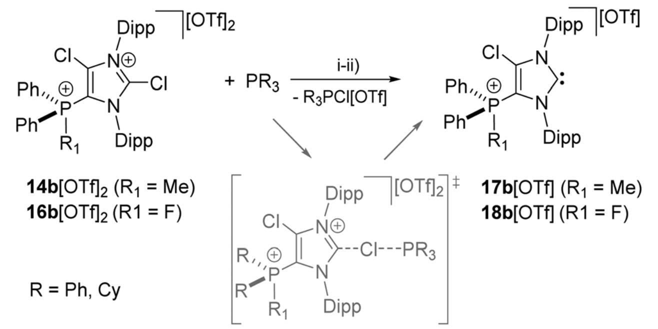

Scheme 5 Preparation of **17b**[OTf], (i): +Cy_3P, C_6H_5F, r.t., 2 h, −Cy_3PCl [OTf], 75%; preparation of **18b**[OTf], (ii): +Ph_3P, C_6H_5F, r.t., 2 h, −Ph_3PCl [OTf], 55%. Proposed transition state of a S_N2(Cl) type reaction (grey).

Similarly, the reaction of **16a,b**[OTf]$_2$ with Ph_3P leads to the quantitative formation of chlorophosphonium salt Ph_3PCl [OTf] (δ(P) = 65.5 ppm)[31] and NHCs **18a,b**[OTf]. The isolation of NHC **18a**[OTf] was hampered due to similar solubility of **18a**[OTf] and PPh_3Cl[OTf]. **18b**[OTf] shows a slightly downfield shifted doublet resonance at δ(P) = 76.8 ppm ($^1J_{PF}$ = 996 Hz) in the ^{31}P NMR spectrum compared to the starting material **15**[OTf]$_2$ (δ(P) = 70.5 ppm). The confirmation of the carbene was given by the $^{13}C\{^1H\}$ NMR spectrum showing a resonance at δ(C) = 230.8 ppm,[16,32] which splits into a *pseudo* triplet ($^3J_{CP}$ = 5 Hz, $^4J_{CF}$ = 5 Hz) due to the coupling to the phosphorus atom and the fluorine atom, respectively. Mechanistically, the formation of NHCs **17a,b**$^+$ and **18a,b**$^+$ proceeds *via* a S_N2(Cl) type reaction[33] which is initiated by the nucleophilic attack of R_3P (R = Ph, Cy) on the σ-hole of the Cl1 atom bonded to the C2-position. This suggestion is supported by a detailed computational study considering a S_N2(Cl) type reaction. The calculations were performed using the high level *ab initio* method RI-MP2[34] with the def2-TZVP[28] basis set to obtain reliable reaction barriers (Fig. 6, left).[29] In initial calculations a minimalistic model was used considering PH_3 as nucleophile which reacts with **14b**$^{2+}$ where the Dipp-substituents are replaced by H atoms. The reaction is initiated by the formation of a hypercoordinate complex **I** in which a P···Cl halogen bond[20] with a comparatively short bond distance of 3.151 Å is observed. This intermediate was found to be 9.2 kcal mol^{-1} lower in energy than the corresponding starting materials and is well organized for the subsequent S_N2(Cl) type reaction[33] as it presents an ideal directionality for the

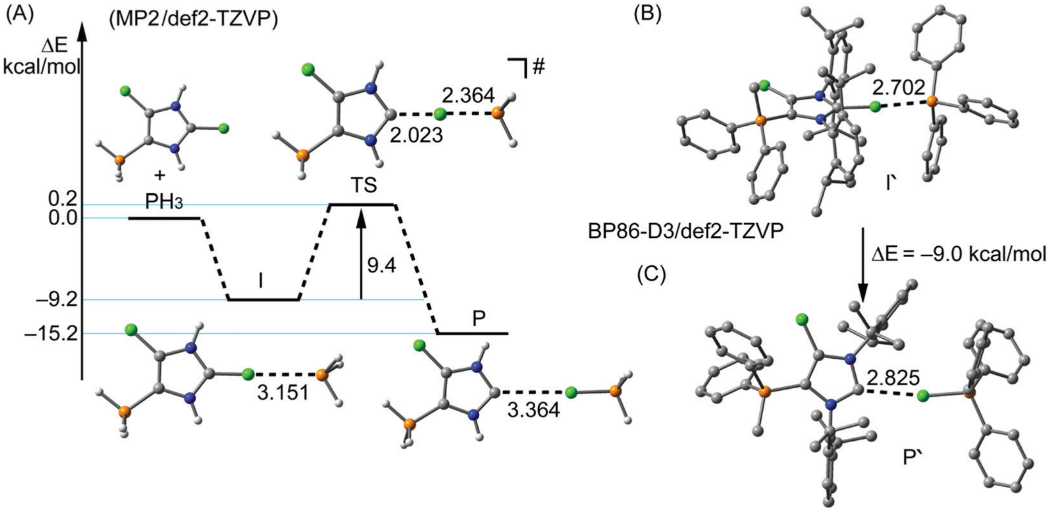

Fig. 6 MP2/def2-TZVP reaction coordinate, energies and geometries of the S_N2(Cl) type reaction (left, A); DFT optimized geometries of the intermediate **I** and products **P** of the experimental system (right, B and C; distances are given in Å).

nucleophilic attack. The transition state **TS** is only 9.4 kcal mol^{-1} higher in energy than the intermediate **I**, thus confirming that the formation of the carbene is energetically feasible. The resulting adduct **P** is 6 kcal mol^{-1} lower in energy than the intermediate **I** and in total 15.2 kcal mol^{-1} more stable than the starting materials. These findings were then transferred to the complete model with dicationic $\mathbf{14b}^{2+}$ and PPh_3 as nucleophile using the density functional theory methods BP86-D3/def2-TZVP[26–29] (Fig. 6, right). The hypercoordinate complex **I′** with a P⋯Cl bond distance of 2.702 Å and the product **P′** were computed. The obtained energy difference between **I′** and **P′** with a value of −9 kcal mol^{-1} is in good agreement with the high level *ab initio* MP2/def2-TZVP calculation of the minimalistic model.

As NHCs are extensively used in coordination chemistry of transition metals, the formation of a series of complexes was investigated. The isolation of transition metal complexes **19**[OTf], **20**[OTf], **21**[OTf] and **23**[OTf] succeeds *via* the *in situ* reaction of compounds **14b**$[OTf]_2$ or **16b**$[OTf]_2$ with R_3P (R = Cy, for **19**[OTf], **20**[OTf], and **23**[OTf]; R = Ph, for **21**[OTf]) in the presence of one equivalent of the corresponding transition metal salts at ambient temperature (Scheme 6; AuCl(tht) for **19**[OTf] and **21**[OTf], CuBr(tht) for **20**[OTf], $[RhCl(cod)]_2$ for **23**[OTf]) in THF. The formation of the complexes is indicated by the $^{13}C\{^1H\}$ NMR spectra of the respective compounds showing resonances at $\delta(C)$ = 183.0 ppm for **19**[OTf], $\delta(C)$ = 186.5 ppm for **21**[OTf], $\delta(C)$ = 189.51 ppm for **20**[OTf] and $\delta(C)$ = 206.03 ppm for **23**[OTf].[16] The reaction of **14b**$[OTf]_2$ with Cy_3P and one eq. AgOTf in THF leads to the formation of **22**$[OTf]_3$ which is a rare example of a tricationic bis-carbene silver complex.[35] The investigation of the NMR spectra of isolated **22**$[OTf]_3$ show only one set of resonances (*e.g.* $\delta(C)$ = 186.5 ppm, d, $^1J_{CAg107}$ = 202 Hz, $^1J_{CAg109}$ = 234 Hz; $\delta(P)$ = 14.1 ppm), indicating a symmetric arrangement of the two ligands around the Ag atom. Single crystals suitable for X-ray crystallography of the triflate salt of $\mathbf{22}^{3+}$ are obtained by slow diffusion of Et_2O into a saturated CH_3CN solution (Fig. 7). The Ag atom is in an almost linear arrangement between the two

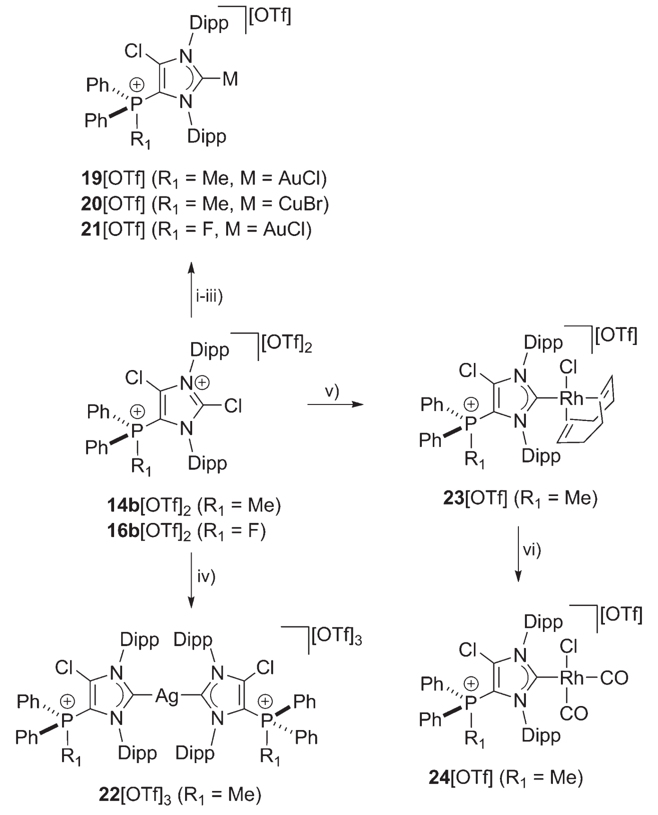

Scheme 6 Preparation of: **19**[OTf], (i): $+Cy_3P$, +AuCl(tht), THF, r.t., 2 h, $-[Cy_3PCl][OTf]$, −tht, 88%; **20**[OTf], (ii): $+Cy_3P$, +CuBr(tht), THF, r.t., 2 h, $-[Cy_3PCl][OTf]$, −tht, 93%; **21**[OTf], (iii): $+Ph_3P$, +AuCl(tht), THF, 2 h, $-[Ph_3PCl][OTf]$, −tht, 87%; **22**$[OTf]_3$, (iv): $+Cy_3P$, +AgOTf, THF, r.t., 4 h, $-[Cy_3PCl][OTf]$, 82%; **23**[OTf], (v): $+Cy_3P$, $+RhCl(cod)_2$, THF, r.t., $[Cy_3PCl][OTf]$, −cod, 88%; **24**[OTf], (vi): +2CO, CH_2Cl_2, r.t., 1.5 h, −cod, 86%.

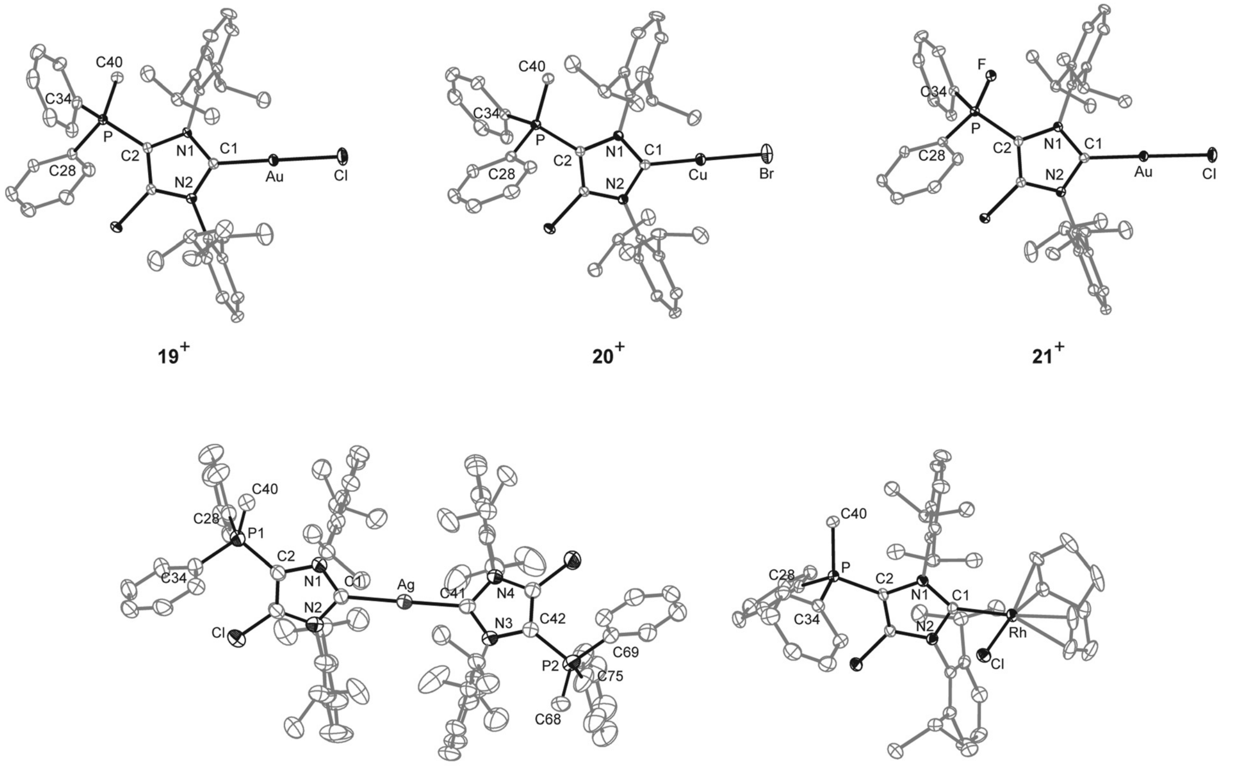

19^+ 20^+ 21^+

22^{3+} 23^+

Fig. 7 Molecular structures of 19^+, 20^+, 21^+, 22^{3+} and 23^+ of the respective triflate salts; hydrogen atoms, solvent molecules and anions are omitted for clarity and thermal ellipsoids are displayed at 50% probability. Selected geometrical parameters are given in Tables 1 and 2.

Table 1 Selected geometrical parameters of crystallographically characterized cations $\mathbf{14b}^{2+}$, $\mathbf{17b}^{+}$, $\mathbf{19}^{+}$, $\mathbf{20}^{+}$, $\mathbf{22}^{3+}$ and $\mathbf{23}^{+}$

	$\mathbf{14b}^{2+}$	$\mathbf{17b}^{+}$	$\mathbf{19}^{+}$	$\mathbf{20}^{+}$	$\mathbf{22}^{3+\,c}$	$\mathbf{23}^{+}$
P–C2 in Å	1.810(2)	1.779(2)	1.794(3)	1.788(2)	1.792	1.785(2)
P–C28 in Å	1.782(2)	1.785(5)	1.780(3)	1.783(2)	1.787	1.795(2)
P–C34 in Å	1.787(2)	1.790(2)	1.772(3)	1.782(2)	1.80	1.792(2)
P–C40 in Å	1.790(2)	1.785(2)	1.782(3)	1.787(3)	1.790	1.786(2)
C1–N1 in Å	1.335(2)	1.375(3)	1.350(4)	1.346(3)	1.359	1.360(3)
C1–N2 in Å	1.337(2)	1.362(3)	1.354(4)	1.365(3)	1.358	1.380(3)
C1–M^a in Å	—	—	1.981(3) (M = Au)	1.884(2) (M = Cu)	2.139 (M = Ag)	2.039(2) (M = Rh)
N1–C1–N2 in (°)	110.42(14)	102.40(16)	106.2(3)	104.81(19)	104.35	104.78(19)
C1–M–X^b in (°)	—	—	176.75(10) (X = Cl)	174.88(7) (X = Br)	178.27(15) (X = C)	86.85(6) (X = Cl)
Cl1···O$_{\text{triflate}}$ in Å	2.813(2)	—	—	—	—	—

^{a} M = transition metal. ^{b} X = halogen atom. ^{c} Average bond lengths and angles are given.

carbenes (C1–Ag–C41 178.27(15)°) but the NHC ligands are slightly twisted as illustrated by the torsion angle of N1–C1–C41–N3 34.380°. Molecular structures of the transition metal complexes $\mathbf{19}^{+}$, $\mathbf{20}^{+}$, $\mathbf{21}^{+}$, $\mathbf{22}^{3+}$ and $\mathbf{23}^{+}$ are depicted in Fig. 7 and selected geometrical parameters are given in Tables 1 or 2. As expected, the average N1–C1–N2 bond angles of cationic NHC complexes (N1–C1–N2: range of 103.2(3)°–106.2(3)°) are wider than the corresponding bond angle in free cationic NHC $\mathbf{17b}^{+}$ (N1–C1–N2 102.40(16)°).[16,35] Accordingly, the N1–C1/N2–C1 bond lengths in complexes $\mathbf{19}^{+}$, $\mathbf{20}^{+}$, $\mathbf{21}^{+}$, $\mathbf{22}^{3+}$, $\mathbf{23}^{+}$ (N1–C1/N2–C1: range of 1.346(3) Å–1.366(3) Å) are slightly shortened compared to those in $\mathbf{17b}^{+}$ (av. N1–C1/N2–C1 1.369 Å), which

Table 2 Selected geometrical parameters of crystallographically characterized cations $\mathbf{15b}^{+}$, $\mathbf{16b}^{2+}$ and $\mathbf{21}^{+}$

	$\mathbf{15b}^{+}$	$\mathbf{16b}^{2+}$	$\mathbf{21}^{+}$
P–C2 in Å	1.826(3)	1.782(3)	1.774(3)
P–C28 in Å	1.808(3)	1.778(3)	1.754(3)
P–C34 in Å	1.804(3)	1.769(3)	1.748(3)
P–F1 in Å	1.6523(19)	1.561(2)	1.5422(17)
P–F2 in Å	1.6582(19)	—	—
C1–N1 in Å	1.332(4)	1.320(3)	1.350(3)
C1–N2 in Å	1.334(4)	1.335(3)	1.366(3)
C1–Au in Å	—	—	1.973(2)
N1–C1–N2 in (°)	109.5(2)	110.0(2)	105.2(2)
C1–Au–Cl in (°)	—	—	177.74(8)

is also in line with the coordination to transition metals.[16] The C1–metal bond lengths in cationic complexes **19**$^+$, **20**$^+$, **21**$^+$, **22**$^{3+}$, and **23**$^+$ are comparable to those observed in other neutral NHC metal complexes.[35,36]

In order to elucidate the donor/acceptor properties of cationic NHC **17b**[OTf], we synthesized the *cis*-chlorodicarbonylrhodium complex **24**[OTf] *via* the reaction of carbon monoxide with **23**[OTf] (Scheme 6)[29] and subsequently investigated the IR stretching frequencies for the carbonyl ligands of the formed carbonyl complex (see Fig. S2.10†). The average CO stretching frequency (ν_{av}(CO) = 2040.3 cm^{-1}, TEP = 2051 cm $^{-1}$)[18] indicate a weak donor ability of cationic NHC **17b**[OTf]. According to a recent work by Ganter and co-workers, the $^1J_{CH}$ coupling constant in imidazolium salts correlates with the σ-donor strength of the corresponding carbene.[37] It was found that poor σ-donors reveal high coupling constants for the C–H bond, which can be explained by a higher s-orbital character of the corresponding C–H bond[38] (compare [Im^{Mes}-H]$^{+}$:[39] $^1J_{CH}$ = 206 Hz and [4,5-Cl-Im^{Dipp}-H]$^+$: $^1J_{CH}$ = 229 Hz).[37] For imidazolium salt **17bH**$^{2+}$ (**17b**$^+$ protonated at C1), we observed a $^1J_{CH}$ coupling constant of 233 Hz (see Fig. S2.2†)[29] rendering cationic NHC **17b**$^+$ a weak σ-donor. We thus conclude that our cationic NHCs are very electron deficient (weak σ-donor), which is promising for interesting follow up chemistry (*vide infra*).

The ambiphilic nature of **18b**$^+$ is displayed by the reaction of **18b**[OTf] with silver fluoride (AgF) in a 1 to 1 stoichiometry at ambient temperature in C_6H_5F yielding complex **25**[OTf] (Scheme 7). The ^{31}P NMR spectrum of **25**[OTf] shows a triplet resonance at δ(P) = −65.3 ppm ($^1J_{PF}$ = 701 Hz) indicating a clean formation of cation **25**$^+$ (see Fig. S2.3†). Additionally, the ^{13}C{^{1}H} NMR spectrum shows two doublets at δ(C) = 184.3 ppm ($^1J_{CAg109}$ = 232 Hz, $^1J_{CAg107}$ = 200 Hz; see Fig. S2.4†), indicative for the coordination of carbene to the silver atom.[35]

25[OTf] is extremely sensitive and decomposes readily in solution which prevents its isolation. In 2010 Bertrand and co-workers reported on the activation of the primary phosphane $PhPH_2$ using NHC **26**[39] and isolated the insertion product of the oxidative addition **27** in high yield (Scheme 8I).[39] Only recently, Radius and co-workers reported on the dehydrogenative coupling of primary and secondary phosphanes utilizing the more electron deficient NHC **28** (Scheme 8II).[40] For the 1 to 2 reaction of **28** with Ph_2PH an oxidative addition of the phosphane into the carbene moiety followed by a reductive elimination of the corresponding diphosphane and the 2,3-dihydro-1*H*-imidazole **29** was assumed.[40]

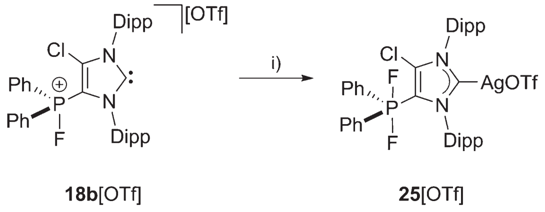

Scheme 7 Reaction of **18b**[OTf] with AgF: (i) C_6H_5F, r.t., 10 h.[29]

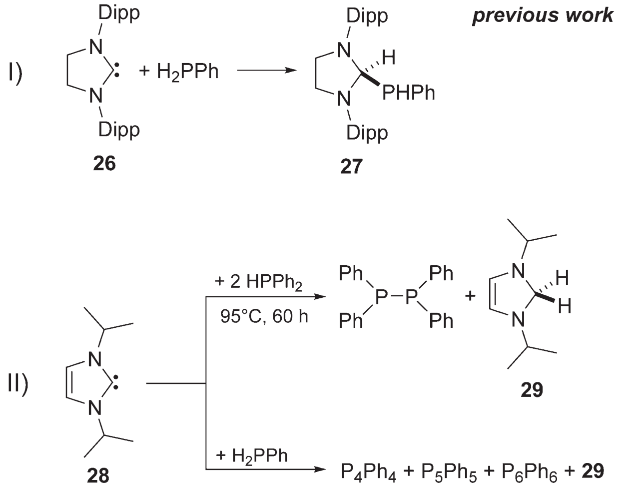

Scheme 8 Reaction of **26** with H_2PPh (I) and dehydrocoupling reactions of $HPPh_2$ or H_2PPh with **28** (II).

Similarly, the reaction of prim. and sec. phosphanes with the electron deficient cationic NHC **17b**$^+$ was performed. The reaction of two equivalents Ph_2PH with **17b**$^+$ in 1,2-dichloroethane (DCE) at ambient temperature affords the quantitative formation of diphosphane Ph_4P_2 after 12 h (Scheme 9,

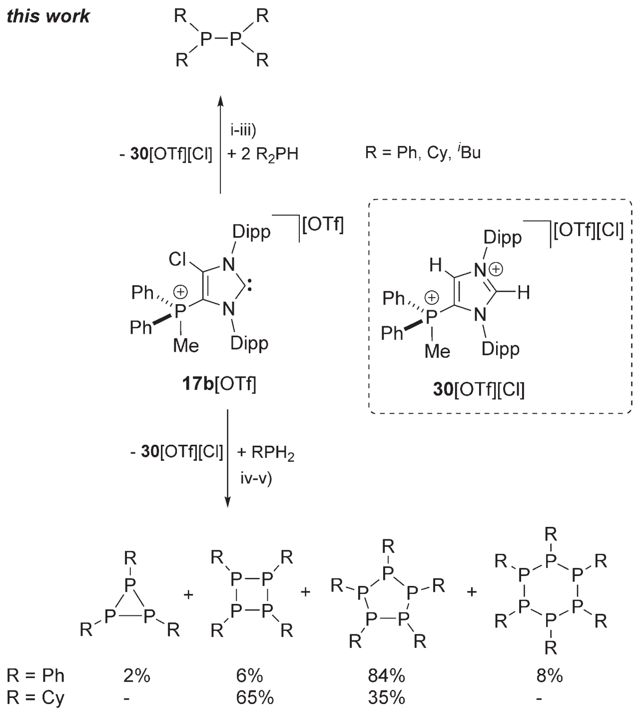

Scheme 9 P–P coupling reactions of R_2PH (R = Ph, Cy, ^{i}Bu; top) and $PhPH_2$ (bottom) using **17b**[OTf] as hydrogen acceptor; (i) +2 eq. Ph_2PH, DCE, r.t., 12 h; (ii) +2 eq. Cy_2PH, CH_3CN, r.t., 12 h; (iii) +2 eq. $^i Bu_2PH$, CH_3CN, r.t., 10 h; (iv) +$PhPH_2$, r.t., 10 h, product distribution estimated by integration of the ^{31}P NMR spectrum of the reaction mixture; (v) +$CyPH_2$, r.t., 24 h, product distribution estimated by integration of the ^{31}P NMR spectrum of the isolated solid.

Fig. S2.5†). The ^{31}P NMR spectrum of the reaction mixture shows a singlet resonance at δ(P) = −16.3 ppm which can be attributed to Ph_4P_2 [40] and a singlet at δ(P) = 12.1 ppm, corresponding to the byproduct which is formed during the reaction. To our surprise, in depth NMR spectroscopic studies reveal dication **30**$^{2+}$ as byproduct of this reaction and not the corresponding 2,3-dihydro-1*H*-imidazole. It was reported that aryl substituents at the phosphane are beneficial for the NHC mediated[40,41] or transition metal catalysed[42] dehydrocoupling reaction, since electron rich alkyl phosphanes gave either no, or a non-selective conversion.

When alkyl phosphanes R_2PH (R = Cy, ^{i}Bu) are reacted with **17b**[OTf] in a 2 to 1 stoichiometry in CH_3CN at ambient temperature, a clean formation of the corresponding diphosphane R_4P_2 (R = Cy, ^{i}Bu) is observed after 10 h reaction time. The reaction of 2 eq. Cy_2PH with **17b**[OTf] in CH_3CN leads to the formation of a colorless precipitate. The ^{31}P NMR spectrum of the isolated precipitate reveals a singlet resonance at δ(P) = −21.3 ppm illustrating a clean and quantitative formation of diphosphane Cy_4P_2 (see Fig. S2.6†). The ^{31}P NMR spectrum for the reaction of 2 eq. ^{i}Bu$_2$PH with **17b**[OTf] shows a singlet at δ(P) = 13.5 ppm for **30**$^{2+}$ and a singlet resonance at δ(P) = −52.4 ppm which is attributed to ^{i}Bu$_4$P$_2$. Small amounts of unreacted ^{i}Bu$_2$PH give rise to a doublet resonance at δ(P) = −83.7 ppm due to a slight excess of the inserted phosphane in the reaction (see Fig. S2.7†). No conversion is observed when 2 eq. of the more sterically encumbered ^{t}Bu$_2$PH is reacted with **17b**[OTf], leading to the assumption that the dehydrogenative coupling reaction maybe limited by the steric demand but not necessarily by electronic effects of the corresponding substituents on the phosphane.

The equimolar reaction of cationic NHC **17b**$^+$ with primary phosphane $PhPH_2$ in 1,2-dichloroethane at ambient temperature led to the formation of *cyclo*-phosphanes Ph_3P_3, Ph_4P_4, Ph_5P_5 and Ph_6P_6 (>90%) along with small amounts of unidentified side products and imidazolium dication **30**$^{2+}$. The proton decoupled ^{31}P NMR spectrum of the reaction mixture revealed an approximate product distribution of the *cyclo*-phosphanes of which Ph_5P_5 (*ca.* 84%) is found to be the main product (see Fig. S2.8†). Reacting the alkyl phosphane $CyPH_2$ with **17b**[OTf] in a 1 : 1 stoichiometry in CH_3CN afforded the quantitative precipitation of Cy_4P_4 and Cy_5P_5 after 24 h. The ^{31}P NMR spectrum of the isolated solid shows two singlet resonances which are assigned to Cy_4P_4 (δ(P) = −68.8 ppm,[43] 65%) and Cy_5P_5 (δ(P) = 7.7 ppm,[44] 35%; see Fig. S2.9†), illustrating that NHC **17b**$^+$ is also suitable for the dehydrocoupling of prim. phosphanes to *cyclo*-phosphanes.

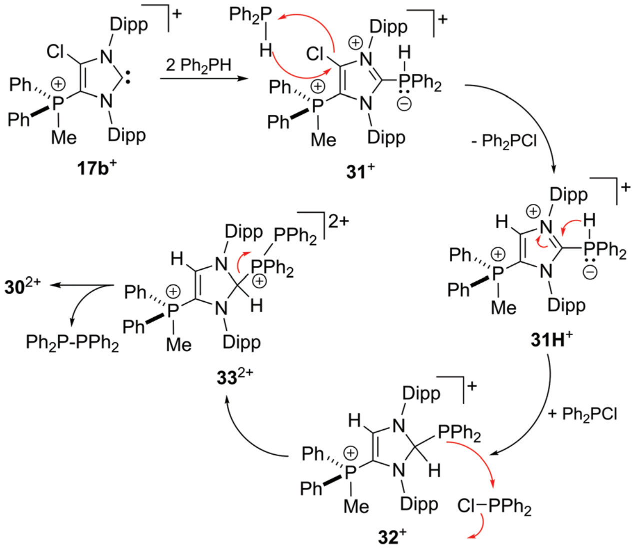

Scheme 10 Possible reaction mechanism for the P–P coupling reaction of 2 eq. R_2PH with **17b**$^+$ to R_2P–PR_2.

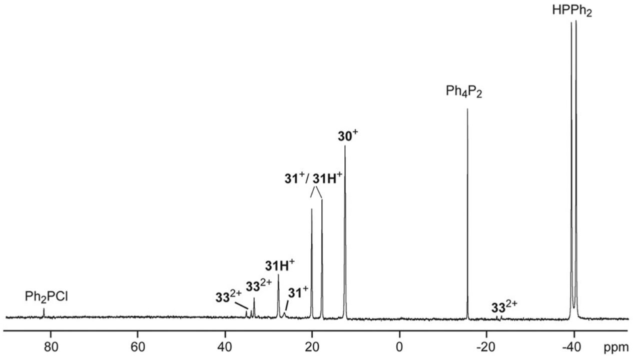

Fig. 8 ^{31}P NMR spectrum for the reaction of **17b**[OTf] with 5 eq. Ph_2PH after 8 h (1,2-dichloroethane, C_6D_6-capillary, 300 K). Resonances are assigned to possible intermediates for the mechanism of the P–P coupling reaction.

To support a possible reaction mechanism (Scheme 10), 5 eq. of Ph_2PH and **17b**[OTf] were mixed together in DCE and the reaction mixture was investigated by means of ^{31}P NMR spectroscopy (Fig. 8). We assume that the first step of this reaction involves the nucleophilic attack of cation **17b**$^+$ towards Ph_2PH to give the hyper-coordinate intermediate **31**$^+$. Related phosporanides were recently reported.[1g,5] This intermediate reacts with a second eq. of Ph_2PH to **31H**$^+$, accompanied by the formation of Ph_2PCl (δ(P) = 81.8 ppm).[13] Cation **31H**$^+$ shows a doublet resonance due to proton coupling at δ(P) = 18.9 ppm ($^1J_{PH}$ = 477 Hz) and a singlet at δ(P) = 27.6 ppm for the tetra-coordinate phosphorus atom. Small amounts of cation **31**$^+$ are present in the spectrum as indicated by the observation of a singlet of low intensity at δ(P) = 26.4 ppm. The corresponding doublet for the penta-coordinate P-atom coincides with that of **31H**$^+$. Intermediate **31H**$^+$ rearranges to 2,3-dihydro-1*H*-imidazole **32**$^+$ in accordance to the work by Bertrand, Röschenthaler and Radius.[1g,39,40] This cation readily reacts with the liberated Ph_2PCl to dication **33**$^{2+}$ which is indicated by the observation of two doublets at δ(P) = −23.4 ppm and δ(P) = 34.6 ($^1J_{PP}$ = −227 Hz) and a singlet resonance at δ(P) = 33.3 ppm for the phosphonium moiety in the backbone. In the last step, cation **33**$^{2+}$ liberates Ph_4P_2 accompanied by the formation of dication **30**$^{2+}$.

Further reactivity studies of **17b**[OTf] were directed towards the synthesis of a cationic N-heterocyclic olefin (NHO).[45,46] Therefore we methylated in a first step the *in situ* formed cation $\mathbf{17b}^+$ obtained from **14b**$[\mathrm{OTf}]_2$ and Cy_3P with one equivalent of MeOTf to give dication $\mathbf{34}^{2+}$ (Scheme 11). Dication $\mathbf{34}^{2+}$ was isolated as triflate salt (isolated yield 91%) and investigated by means of multinuclear NMR spectroscopy and X-ray analysis (Fig. 9). The ^{1}H NMR spectrum of dissolved **34**$[\mathrm{OTf}]_2$ in CD_2Cl_2 reveals a doublet resonance at $\delta(\mathrm{H}) = 2.91$ ppm ($^2J_{\mathrm{HP}} = 13.8$ Hz) for the CH_3-group which is bonded to the phosphorus atom whereas the CH_3-group at the 2-position of the imidazolium ring gives a singlet resonance at $\delta(\mathrm{H}) = 2.38$ ppm. The ^{31}P NMR spectrum shows a quartet resonance at $\delta(\mathrm{P}) = 15.6$ ppm which is slightly upfield shifted compared to $\mathbf{14b}^{2+}$ ($\delta(\mathrm{P}) = 16.9$ ppm). Derivative **34**$[\mathrm{OTf}]_2$ is readily deprotonated in a subsequent step by lithium diisopropylamide (LDA) in THF to give **35**[OTf] as yellow powder in excellent yield (93%). The ^{31}P NMR spectrum shows an upfield shifted quartet resonance at $\delta(\mathrm{P}) = 9.6$ ppm compared to dication $\mathbf{34}^{2+}$ ($\delta(\mathrm{P}) = 15.6$ ppm).

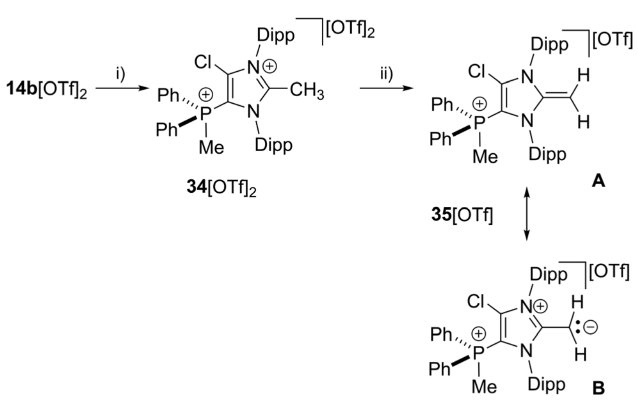

Scheme 11 Preparation of **34**$[\mathrm{OTf}]_2$, (i) $+Cy_3P$, MeOTf, C_6H_5F, r.t., 14 h, $-Cy_3PCl[OTf]$, 91%; and **35**[OTf], (ii) +LDA THF, r.t., 30 min, −Li[OTf], −HDA (diisopropylamine), 93%; two representative resonance structures (**A**, **B**) of **35a**[OTf] are displayed.

The doublet resonance for the CH_3-group bound to the P atom is shifted to higher field ($\delta(\mathrm{H}) = 1.83$ ppm; $^2J_{\mathrm{HP}} = 13.6$ Hz) compared to the corresponding CH_3-group in $\mathbf{34}^{2+}$ ($\delta(\mathrm{H}) = 2.91$ ppm; $^2J_{\mathrm{HP}} = 13.8$ Hz). The CH_2-group at the 2-position of the imidazole ring gives rise to a doublet resonance at $\delta(\mathrm{H}) = 2.54$ ppm and a doublet of doublet resonance at $\delta(\mathrm{H}) = 2.61$ ppm due to the hindered rotation around the C1–CH_2 bond. Both signals exhibit a geminal coupling constant of $^2J_{\mathrm{HH}} = 3.7$ Hz and the latter resonance shows an additional coupling to the P atom ($^5J_{\mathrm{HP}} = 1.6$ Hz) which is explained by the spatial arrangement of this proton (see Fig. S2.11†). The C atom of the CH_2-group resonates at $\delta(\mathrm{P}) = 55.1$ ppm which is in the typical range for an olefinic C atom. Single crystals suitable for X-ray crystallography are obtained by slow diffusion of Et_2O into a saturated solution of **35**[OTf] in CH_3CN at −35 °C (Fig. 9). Compared to the molecular structure of $\mathbf{34}^{2+}$ the major differences are the elongated C1–N1/N2 bond distances (C1–N1 1.404(3) Å, C1–N2 1.399(3) Å in $\mathbf{35}^+$ and C1–N1 1.347(5) Å, C1–N2 1.332(5) Å) in $\mathbf{34}^{2+}$) and the reduced bond angle between N1–C1–N2 (104.6(2)° in $\mathbf{35}^+$ and N1–C1–N2 109.141(9)° in $\mathbf{34}^{2+}$) and are explained by a diminished degree of π-delocalization between the N1–C1–N2 moiety and an increased p-orbital character of the C1–N1/N2 bonds. The C1–C4 bond length of 1.334(4) Å is well within the range of a typical olefinic C═C double bond (1.34 Å).[47] Cation $\mathbf{35}^+$ is regarded as cationic N-heterocyclic olefin (NHO) of which the main resonance structures (**A**, **B**) are depicted in Scheme 11, indicating the highly polarized nature of the exocyclic C═C double bond. As already discussed by others, NHOs are of great interests as strong two-electron donors due to their considerable nucleophilic character.[45,46]

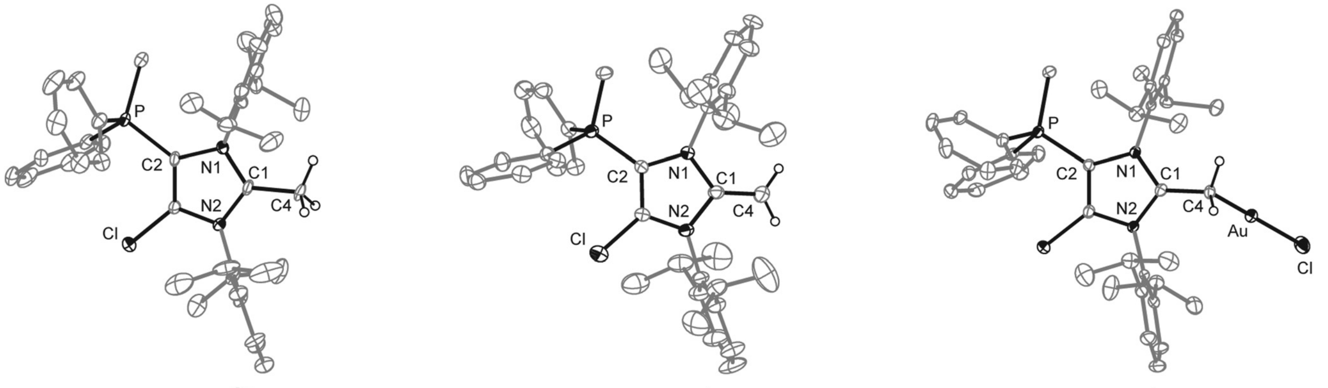

$\mathbf{34}^{2+}$ $\mathbf{35}^{+}$ $\mathbf{36}^{+}$

Fig. 9 Molecular structures of $\mathbf{34}^{2+}$, $\mathbf{35}^+$, and $\mathbf{36}^+$, of the respective triflate salts; hydrogen atoms, solvent molecules and anions are omitted for clarity and thermal ellipsoids are displayed at 50% probability; selected bond lengths (Å) and angles (°) for $\mathbf{34}^{2+}$: C1–C4 1.499(5), C1–N1 1.347(5), C1–N2 1.332(5); N1–C1–N2 109.141(9); $\mathbf{35}^+$: C1–C4 1.334(4), C1–N1 1.404(3), C1–N2 1.339(3); N1–C1–N2 104.6(2); for $\mathbf{36}^+$: C1–C4 1.453(4), C1–N1 1.344(4), C1–N2 1.356(4), C28–Au 2.062(3), Au–Cl 2.3080(8); N1–C1–N2 107.5(3), C1–C4–Au 116.2(2), C4–Au–Cl 174.90(9).

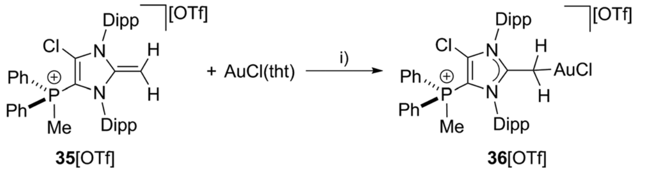

Scheme 12 Preparation of NHO gold complex **36**[OTf]; I) THF, r.t., 3 h, −tht, 78%.

To proof the donor properties of cationic NHO 35^+, the triflate salt was reacted with one equivalent AuCl(tht) in THF at ambient temperature to afford the NHO gold complex **36**[OTf] in good yield (71%, Scheme 12). The ^{31}P NMR spectrum of **36**[OTf] reveals a slightly downfield shifted resonance at δ(P) = 9.6 ppm compared to the free ligand 35^+ (δ(P) = 14.3 ppm). The ^{1}H NMR spectrum of 36^+ shows a singlet resonance for the CH_2-group at δ(H) = 2.36 ppm, thus the two protons of the CH_2 moiety become magnetically equal upon coordination to the transition metal due to the free rotation around the C1–CH_2 bond (see Fig. S2.11†). The coordination of the gold chloride fragment to the CH_2-group causes a pronounced high field shift in the ^{13}C NMR spectrum (δ(C) = 8.5 ppm) compared to cation 35^+ (δ(C) = 55.1 ppm). Single crystals suitable for X-ray crystallography are obtained by slow diffusion of Et_2O into a saturated solution of **36**[OTf] in CH_3CN at −35 °C (Fig. 9). The molecular structure of cation 36^+ displays a tetra-coordinate bonding environment at the C4 atom with a C1–C4–Au bond angle of 116.2(2)° and an elongated C1–C4 bond length of 1.453(4) Å compared to that in 35^+ (C1–C4 1.399(3) Å). This elongation is a result of the reduced π-bond character of the C1–C4 bond caused by the coordination of the gold chloride fragment.

Conclusions

In this contribution, we present a facile and high yielding syntheses of 2-phosphanyl-(**9a**,**b**[OTf]) and 5-phosphanyl-(**10a**,**b**[OTf]) substituted imidazolium salts from the reaction of the corresponding chlorophosphanes and NHC **8**. Methylation or oxidation with XeF_2 and subsequent fluoride abstraction of these salts affords 5-phosphonio substituted imidazolium salts **14a**,**b**$[OTf]_2$ and **16a**,**b**$[OTf]_2$ in good to very good yields. Quantum chemical calculations revealed the Cl1 atom (σ-hole) the most reactive position towards bulky nucleophiles. Chlorenium abstraction is achieved by the addition of R_3P (R = Ph, Cy) in a S_N2(Cl) type reaction to yield the first cationic 5-phosphonio-substituted NHCs **17a**,**b**$^+$ and **18a**,**b**$^+$ as triflate salts. These salts are a new class of electron deficient cationic NHCs which conveniently form transition metal complexes with corresponding metals salts (AuCl(tht) for **19**[OTf], and **21**[OTf], CuBr(tht) for **20**[OTf], $[RhCl(cod)]_2$ for **23**[OTf]) and AgOTf for **22**$[OTf]_3$). As shown for derivative **17b**[OTf], the methylated derivatives can be handled also in solvents such as CH_2Cl_2 and CH_3CN without decomposition which significantly broadens the scope of application. **17b**[OTf] was used in dehydrocoupling reactions of prim. and sec. aryl and even alkyl phosphanes. The preparation of a highly nucleophilic N-heterocyclic olefin (NHO, **35**[OTf]) proceeds *via* a two step synthesis involving the reaction of *in situ* formed **17b**[OTf] with MeOTf and subsequent deprotonation with LDA. Cation 35^+ acts as a two-electron donor as confirmed by the isolation of the AuCl complex **36**[OTf].

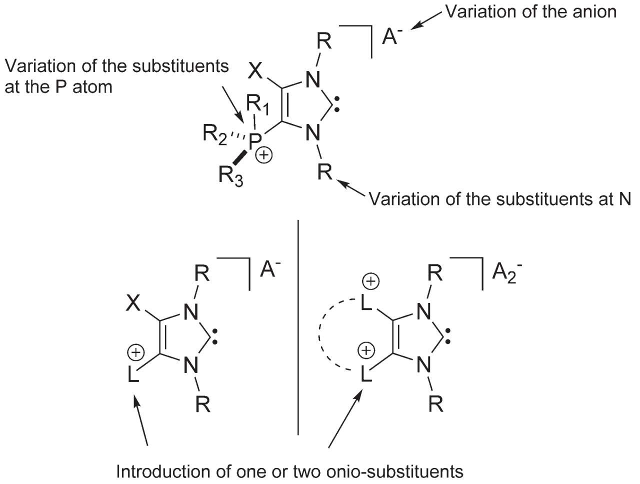

Chart 1 Possible variations for a new class of NHC systems.

The isolation of the first NHC salts does impact the broad field of NHC chemistry since it allows the design of new charged systems (Chart 1). Thus, the opportunity of including a variety of different onio-substituents (phosphanes, amines, pyridines[48] *etc.*)[49] allows for the introduction of additional cationic charges in 4/5-position. This should have a tremendous influence on the reactivity of the resulting carbenes which was already shown by a *in situ* formed pyridinio-substituted NHC derivative.[48] The introduction of a stereogenic center is feasible by the variation of the substituents at the phosphonium center, the substituents of the N atoms in the heterocycle, as well as the choice of counter-ions which makes the resulting systems interesting candidates for stereoselective transition metal or organo catalysis.

Acknowledgements

This work was supported by the Fonds der Chemischen Industrie (FCI, Kekulé scholarship for F. H.), the German Science Foundation (DFG, grant number WE 4621/2-1) and the ERC (ERC starting grant SynPhos: 307616). A. B. and A. F. thank DGICYT of Spain (projects CTQ2014-57393-C2-1-P and CONSOLIDER INGENIO CSD2010-00065, FEDER funds) for funding. We also thank Philipp Lange and Stephen Schulz for experimental assistance.

References

1 Selected examples of P-centered NHC adducts and imidazoliumyl salts: (*a*) N. Kuhn, J. Fahl, D. Bläser and R. Boese, *Z. Anorg. Allg. Chem.*, 1999, **625**, 729; (*b*) A. J. Arduengo III, J. C. Calabrese, A. H. Cowley, H. V. R. Dias, J. R. Goerlich, W. J. Marshall and B. Riegel, *Inorg. Chem.*, 1997, **36**, 2151; (*c*) A. J. Arduengo III, C. J. Carmalt, J. A. C. Clyburne, A. H. Cowley and R. Pyati, *Chem. Commun.*, 1997, 981; (*d*) C. A. Dyker, A. Decken, B. D. Ellis and C. L. B. Macdonald, *Chem. Commun.*, 2005, 1965; (*e*) Y. Wang, Y. Xie, P. Wei, R. B. King, H. F. Schaefer III, P. v. R. Schleyer and G. H. Robinson, *J. Am. Chem. Soc.*, 2008, **130**, 14970; (*f*) Y. Wang, Y. Xie, M. Y. Abraham, R. J. Gilliard Jr., P. Wei, H. F. Schaefer III, P. v. R. Schleyer and G. H. Robinson, *Organometallics*, 2010, **29**, 4778; (*g*) T. Böttcher, B. S. Bassil, L. Zhechkov, T. Heine and G.-V. Röschenthaler, *Chem. Sci.*, 2013, **4**, 77; (*h*) A. Doddi, D. Bockfeld, T. Bannenberg, P. G. Jones and M. Tamm, *Angew. Chem., Int. Ed.*, 2014, **53**, 13568, (*Angew. Chem.*, 2014, **126**, 13786); (*i*) K.-O. Feldmann, F. D. Henne and J. J. Weigand, *J. Am. Chem. Soc.*, 2010, **132**, 16321; (*j*) F. D. Henne, E.-M. Schnöckelborg, K.-O. Feldmann, J. Grunenberg, R. Wolf and J. J. Weigand, *Organometallics*, 2013, **32**, 6674; (*k*) M. H. Holthausen, S. K. Surmiak, P. Jerabek, G. Frenking and J. J. Weigand, *Angew. Chem., Int. Ed.*, 2013, **52**, 11078, (*Angew. Chem.*, 2013, **125**, 11284); (*l*) F. D. Henne, A. T. Dickschat, F. Hennersdorf, K.-O. Feldmann and J. J. Weigand, *Inorg. Chem.*, 2015, **54**, 6849.

2 For reviews see also: (*a*) S. Gaillard and J.-L. Renaud, *Dalton Trans.*, 2013, **42**, 7255; (*b*) Y. Canac, C. Maaliki, I. Abdellah and R. Chauvin, *New J. Chem.*, 2012, **36**, 17.

3 (*a*) J. I. Bates, P. Kennepohl and D. P. Gates, *Angew. Chem., Int. Ed.*, 2009, **48**, 9844, (*Angew. Chem.*, 2009, **121**, 10028); (*b*) P. K. Majhi, K. C. F. Chow, T. H. H. Hsieh, E. G. Bowes, G. Schnakenburg, P. Kennepohl, R. Streubel and D. P. Gates, *Chem. Commun.*, 2016, **52**, 998.

4 D. Mendoza-Espinosa, B. Donnadieu and G. Bertrand, *J. Am. Chem. Soc.*, 2010, **132**, 7264.

5 K. Schwedtmann, M. H. Holthausen, K.-O. Feldmann and J. J. Weigand, *Angew. Chem., Int. Ed.*, 2013, **52**, 14204, (*Angew. Chem.*, 2013, **125**, 14454).

6 J. I. Bates and D. P. Gates, *Organometallics*, 2012, **31**, 4529.

7 D. Mendoza-Espinosa, B. Donnadieu and G. Bertrand, *Chem. – Asian J.*, 2011, **6**, 1099.

8 E. Aldeco-Perez, A. J. Rosenthal, B. Donnadieu, P. Parameswaran, G. Frenking and G. Bertrand, *Science*, 2009, **326**, 556.

9 K. Majhi, S. Sauerbrey, G. Schnakenburg, A. J. Arduengo III and R. Streubel, *Inorg. Chem.*, 2012, **51**, 10408.

10 (*a*) J. Ruiz and A. F. Mesa, *Chem. – Eur. J.*, 2012, **18**, 4485; (*b*) J. Ruiz, A. F. Mesa and D. Sol, *Organometallics*, 2015, **34**, 5129.

11 P. K. Majhi, G. Schnakenburg, Z. Kelemen, L. Nyulaszi, D. P. Gates and R. Streubel, *Angew. Chem., Int. Ed.*, 2013, **52**, 10080, (*Angew. Chem.*, 2013, **125**, 10264).

12 A. J. Arduengo III, F. Davidson, H. V. R. Dias, J. R. Goerlich, D. Khasnis, W. J. Marshall and T. K. Prakasha, *J. Am. Chem. Soc.*, 1997, **119**, 12742.

13 NMR spectra of the purified chlorophosphanes were measured independently.

14 H. Goldwhite, *Introduction to phosphorus chemistry*, Cambridge University Press, Cambridge, 1981.

15 O. Back, M. Henry-Ellinger, C. D. Martin, D. Martin and G. Bertrand, *Angew. Chem., Int. Ed.*, 2013, **52**, 2939, (*Angew. Chem.*, 2013, **125**, 3011).

16 For reviews see: (*a*) T. Dröge and F. Glorius, *Angew. Chem., Int. Ed.*, 2010, **49**, 6940, (*Angew. Chem.*, 2010, **122**, 7094); (*b*) F. E. Hahn and M. C. Jahnke, *Angew. Chem., Int. Ed.*, 2008, **47**, 3122, (*Angew. Chem.*, 2008, **120**, 3166).

17 J. B. Waters and J. M. Goicoechea, *Coord. Chem. Rev.*, 2015, **293–294**, 80.

18 The Tolman Electronic Paramter (TEP) has been employed in transition metal complexes to evaluate the donor abilities of normal and mesoionic NHCs: (*a*) R. A. Kely III, H. Clavier, S. Guidice, N. M. Scott, E. D. Stevens, J. Bordner, I. Samardjiev, C. D. Hoff, L. Cavallo and S. P. Nolan, *Organometallics*, 2008, **27**, 202; (*b*) D. J. Nelson and S. P. Nolan, *Chem. Soc. Rev.*, 2013, **42**, 6723.

19 H. Bondi, *J. Phys. Chem.*, 1964, **68**, 441.

20 P. Metrangolo, F. Meyer, T. Pilati, G. Resnati and G. Terraneo, *Angew. Chem., Int. Ed.*, 2008, **47**, 6114, (*Angew. Chem.*, 2008, **120**, 6206), and references reported therein.

21 (*a*) N. Inamoto and S. Masuda, *Chem. Lett.*, 1982, **11**, 1003; (*b*) F. De Proft, W. Langenaeker and P. Gerlings, *J. Phys. Chem.*, 1993, **97**, 1826.

22 M. Alcarazo, *Chem. – Eur. J.*, 2014, **20**, 7868.

23 M. Holthausen, M. Mehta and D. W. Stephan, *Angew. Chem., Int. Ed.*, 2014, **53**, 6538, (*Angew. Chem.*, 2014, **126**, 6656).

24 (*a*) M. Pérez, L. J. Hounjet, C. B. Caputo, R. Dobrovetsky and D. W. Stephan, *J. Am. Chem. Soc.*, 2013, **135**, 18308; (*b*) C. B. Caputo, L. J. Hounjet, R. Dobrovetsky and D. W. Stephan, *Science*, 2013, **341**, 1374; (*c*) L. J. Hounjet, C. B. Caputo and D. W. Stephan, *Dalton Trans.*, 2013, **42**, 2629; (*d*) M. Holthausen, J. M. Bayne, I. Mallov, R. Dobrovetsky and D. W. Stephan, *J. Am. Chem. Soc.*, 2015, **137**, 7298.

25 (*a*) O. Kühl, *Phosphorus-31-NMR Spectroscopy*, Springer, Berlin, 2008; (*b*) D. G. Gorenstein, *Phosphorus-31 NMR Principles and Applications*, Academic Press. Inc., Cambridge, 1984.

26 (*a*) A. D. Becke, *Phys. Rev. A*, 1988, **38**, 3098; (*b*) J. P. Perdew, *Phys. Rev. B: Condens. Matter*, 1986, **33**, 8822; (*c*) J. P. Perdew, *Phys. Rev. B: Condens. Matter*, 1986, **34**, 7406.

27 S. Grimme, J. Antony, S. Ehrlich and H. Krieg, *J. Chem. Phys.*, 2010, **132**, 154104.

28 F. Weigend and R. Ahlrichs, *Phys. Chem. Chem. Phys.*, 2005, **7**, 3297.

29 For further details see ESI.†

30 A. Bauzá, J. T. Mooibkoek and A. Frontera, *ChemPhysChem*, 2015, **16**, 2496, and references reported therein.

31 For comparison of the chemical shift, $[Cy_3PCl]^+$ and $[Ph_3PCl]^+$ were independently synthesized according to a literature procedure: J. K. Ruff, *Inorg. Chem.*, 1963, **2**, 813.

32 A. J. Arduengo III, R. L. Harlow and M. Kline, *J. Am. Chem. Soc.*, 1991, **113**, 363.

33 R. Weiss and S. Engel, *Angew. Chem., Int. Ed.*, 1992, **31**, 216, (*Angew. Chem.*, 1992, **104**, 239).

34 F. Weigend, M. Häser, H. Patzelt and R. Ahlrich, *Chem. Phys. Lett.*, 1998, **294**, 143.

35 (*a*) P. de Fremont, N. M. Scott, E. D. Stevens and S. P. Nolan, *Organometallics*, 2005, **24**, 2411; (*b*) P. de Frémont, N. Marion and S. P. Nolan, *J. Organomet. Chem.*, 2009, **694**, 551.

36 P. de Frémont, N. M. Scott, E. D. Stevens, T. Ramnial, O. C. Lightbody, C. L. B. Macdonald, J. A. C. Clyburne, C. D. Abernethy and S. P. Nolan, *Organometallics*, 2005, **24**, 6301.

37 K. Verlinden, H. Buhl, W. Frank and C. Ganter, *Eur. J. Inorg. Chem.*, 2015, 2416.

38 H. A. Bent, *Chem. Rev.*, 1961, **61**, 275.

39 G. D. Frey, J. D. Masuda, B. Donnadieu and G. Bertrand, *Angew. Chem., Int. Ed.*, 2010, **49**, 9444, (*Angew. Chem.*, 2010, **122**, 9634).

40 H. Schneider, D. Schmidt and U. Radius, *Chem. Commun.*, 2015, **51**, 10138.

41 S. Molitor, J. Becker and V. H. Gessner, *J. Am. Chem. Soc.*, 2014, **136**, 15517.

42 Selected examples of transition metal catalyzed dehydrogenative coupling of phosphanes: (*a*) V. P. W. Böhm and M. Brookhart, *Angew. Chem., Int. Ed.*, 2001, **40**, 4694, (*Angew. Chem.*, 2001, **113**, 4832); (*b*) A. K. King, A. Buchard, M. F. Mahon and R. L. Webster, *Chem. – Eur. J.*, 2015, **21**, 15960.

43 A. Henderson Jr., M. Epstein and F. S. Seichter, *J. Am. Chem. Soc.*, 1963, **85**, 2462.

44 J. D. Masuda, A. J. Hoskin, T. W. Graham, C. Beddie, M. C. Fermin, N. Etkin and D. W. Stephan, *Chem. – Eur. J.*, 2006, **12**, 8696.

45 (*a*) N. Kuhn, H. Bohnen, J. Kreutzberg, D. Bläser and R. Boese, *J. Chem. Soc., Chem. Commun.*, 1993, 1136; (*b*) S. M. I. Al-Rafia, A. C. Malcolm, S. K. Liew, M. J. Ferguson, R. McDonald and E. Rivard, *Chem. Commun.*, 2011, **47**, 6987; (*c*) A. C. Malcolm, K. J. Sabourin, R. McDonald, M. J. Ferguson and E. Rivard, *Inorg. Chem.*, 2012, **51**, 12905; (*d*) S. M. I. Al-Rafia, M. R. Momeni, M. J. Ferguson, R. McDonald, A. Brown and E. Rivard, *Angew. Chem., Int. Ed.*, 2013, **52**, 6390, (*Angew. Chem.*, 2013, **125**, 6518); (*e*) Y. Wang, M. Y. Abraham, R. J. Gilliard Jr., D. R. Sexton, P. Wei and G. H. Robinson, *Organometallics*, 2013, **32**, 6639; (*f*) R. S. Ghadwal, S. O. Reichmann, F. Engelhardt, D. M. Andrada and G. Frenking, *Chem. Commun.*, 2013, **49**, 9440; (*g*) S. M. I. Al-Rafia, M. R. Momeni, M. J. Ferguson, R. McDonald, A. Brown and E. Rivard, *Organometallics*, 2013, **32**, 6201; (*h*) S. Kronig, P. G. Jones and M. Tamm, *Eur. J. Inorg. Chem.*, 2013, 2301; (*i*) A. Fürstner, M. Alcarazo, R. Goddard and C. W. Lehmann, *Angew. Chem., Int. Ed.*, 2008, **120**, 3254, (*Angew. Chem.*, 2008, **120**, 3254).

46 For a review of NHOs see: E. Rivard, *Dalton Trans.*, 2014, **43**, 8577; and references reported therein.

47 W. M. Haynes, D. R. Lide and T. J. Bruno, *Handbook of Chemistry and Physics*, CRC Press, New York, 96th edn, 2015.

48 H. Buhl and C. Ganter, *Chem. Commun.*, 2013, **49**, 5417.

49 For transition metal-substituted derivatives see: (*a*) B. Hildebrandt, W. Frank and C. Ganter, *Organometallics*, 2011, **30**, 3483; (*b*) B. Hildebrandt, S. Raub, W. Frank and C. Ganter, *J. Organomet. Chem.*, 2012, **717**, 83; B. Hildebrandt, S. Raub, W. Frank and C. Ganter, *Chem. – Eur. J.*, 2012, **18**, 6670.